

A Comparative Analysis of Machine Learning and Graph-Based Deep Learning Models for MRI-Based ADHD Subtype Classification

Neema. H.N

Research Scholar, Dept of CA, CS & IT, Karpagam Academy of Higher Education, Coimbatore-641021, India.

Dr. N.V. Balaji

Professor & Director, Centre for Continuing Professional Development, Karpagam Academy of Higher Education, Coimbatore-641021, India.

ABSTRACT

Attention Deficit Hyperactivity Disorder (ADHD) is a neurodevelopmental condition characterized by diverse behavioral manifestations and subtle structural variations in the brain. Accurate classification of ADHD subtypes using neuroimaging remains challenging due to high intra-class similarity and limited discriminative features. This study presents a comprehensive comparative analysis of Machine Learning (ML) and Graph-based Deep Learning (DL) models for MRI-based ADHD subtype classification. Structural Magnetic Resonance Imaging (sMRI) data are processed to extract region-specific features from the Caudate Nucleus (CN), incorporating texture, intensity, and morphological characteristics. These features are utilized across multiple classification paradigms, including K-Nearest Neighbor (KNN), Binary-Coded Genetic Algorithm with optimized Extreme Learning Machine (BCGA-ELM), and a semi-supervised Fuzzy C-Means with Advanced Linear Discriminant Analysis (FCM-ALDA). In addition, a Multi-View Graph Attention Transformer Network (MV-GATNet) is employed to capture complex inter-sample relationships and global feature dependencies. The performance of all models is systematically evaluated using Accuracy, Sensitivity, and Specificity metrics. Experimental findings reveal a consistent improvement in classification performance from conventional methods to advanced graph-based DL approaches. In particular, the integration of multi-view representations with attention-driven learning mechanisms significantly enhances subtype discrimination. This study provides a structured evaluation of different learning paradigms and highlights the effectiveness of graph-based models in handling complex neuroimaging data. These insights contribute toward the development of reliable and automated diagnostic support systems for ADHD subtype identification.

Keywords: ADHD Classification; Magnetic Resonance Imaging; Caudate Nucleus; Machine Learning; Graph Attention Networks; Transformer Models

1. INTRODUCTION

ADHD is a prevalent neurodevelopmental disorder characterized by persistent patterns of inattention, hyperactivity, and impulsivity that interfere with cognitive functioning and behavioral regulation [1]. According to recent global health reports, ADHD affects a significant proportion of children worldwide and often persists into adulthood, impacting academic performance, social interactions, and overall quality of life [2]. Clinically, ADHD is categorized into three primary subtypes: Inattentive (ADHD-I), Hyperactive/Impulsive (ADHD-HI), and Combined (ADHD-C), each exhibiting distinct behavioral and neurological characteristics. However, accurate identification of these subtypes remains challenging due to overlapping symptoms and the subjective nature of traditional diagnostic approaches [3]. In recent years, neuroimaging techniques such as MRI have gained significant attention for their potential to provide objective insights into brain structure and function. sMRI enables detailed visualization of brain regions associated with attention control and executive functioning [4]. Among these regions, the CN has been widely studied due to its involvement in motor regulation, cognitive processing, and behavioral control, all of which are closely linked to ADHD pathology. Subtle variations in the morphology and intensity patterns of the CN have been reported across ADHD subtypes, motivating the use of MRI-based computational methods for automated classification [5].

ML techniques have been extensively explored for ADHD classification using neuroimaging data. Traditional approaches such as KNN rely on distance-based similarity measures to classify samples based on feature proximity [6]. While these methods are simple and computationally efficient, they often struggle with high-dimensional data and complex feature distributions. To address these limitations, optimized learning frameworks such as BCGA-ELM have been proposed. These models enhance classification performance by optimizing network parameters and improving generalization capabilities. Despite these advancements, purely supervised learning approaches remain dependent on large labeled datasets, which are often limited in medical imaging domains [7]. To overcome the scarcity of labeled data, semi-supervised learning methods have been introduced, enabling the integration of unlabeled data into the training process. Techniques such as FCM-ALDA incorporate clustering and discriminant learning to improve class separability while leveraging unlabeled samples. These approaches have demonstrated improved performance in scenarios with limited labeled data; however, they are still constrained in capturing complex nonlinear relationships and global feature dependencies inherent in neuroimaging data [8].

With the advancement of DL, more sophisticated models have been developed to address these challenges. Convolutional Neural Networks (CNNs) and autoencoder-based frameworks have been applied to extract hierarchical features from MRI and functional MRI (fMRI) data, leading to improved classification accuracy [9]. Nevertheless, these models primarily focus on local feature extraction and may not fully exploit the relational structure between samples. Recent developments in graph-based learning have introduced Graph Neural Networks (GNNs), which model data as nodes and edges to capture inter-sample relationships. In particular, Graph Attention Networks (GAT) have shown promise by assigning adaptive importance to neighboring nodes, enabling more effective representation learning [10]. Furthermore, Transformer-based architectures have emerged as powerful tools for modeling global dependencies through self-attention mechanisms. By capturing long-range interactions, Transformers complement graph-based methods, providing a comprehensive understanding of both local and global patterns in data. The integration of multi-view learning, graph attention mechanisms, and transformer-based modeling offers a promising direction for improving ADHD subtype classification performance.

Given the diversity of available computational approaches, a systematic comparative analysis is essential to understand their strengths and limitations. Evaluating classical machine learning, optimized learning, semi-supervised methods, and advanced DL models under a unified framework can provide valuable insights into their effectiveness for MRI-based ADHD classification. Such analysis not only facilitates the identification of suitable models for clinical applications but also highlights the importance of incorporating relational and contextual learning mechanisms in neuroimaging analysis.

Problem Statement: Despite significant advancements in computational neuroimaging, accurate classification of ADHD subtypes remains a challenging task due to subtle structural variations, high intra-class similarity, and limited availability of labeled datasets. Traditional ML models often fail to capture complex feature interactions, while advanced models may require large-scale data and computational resources. Additionally, the lack of a unified evaluation framework makes it difficult to assess the relative effectiveness of different approaches. Therefore, there is a need for a systematic comparative analysis of diverse learning models to identify their strengths, limitations, and suitability for MRI-based ADHD subtype classification.

Paper Contributions: This study presents a comprehensive comparative analysis of multiple computational approaches for ADHD subtype classification using MRI data. First, region-specific features are extracted from the CN, incorporating texture, intensity, and shape characteristics. Second, the study evaluates the performance of classical ML (KNN), optimized learning (BCGA-ELM), and semi-supervised methods (FCM-ALDA) under a unified experimental setup. Third, a graph-based DL model incorporating attention mechanisms and global contextual learning is analyzed to understand its effectiveness in capturing complex relationships. Fourth, the models are systematically compared using standardized

performance metrics, including Accuracy, Sensitivity, and Specificity. Finally, the study provides insights into the progression of learning paradigms and their impact on classification performance in neuroimaging applications.

Paper Organization: The remainder of this paper is structured as follows: Section 2 reviews recent literature related to ADHD classification using ML and DL approaches. Section 3 describes the methodologies, including feature extraction, model architectures, and a comparative framework. Section 4 presents the experimental results and comparative analysis. Finally, Section 5 concludes the study and outlines potential directions for future research.

2. RELATED WORKS

Recent advancements in ADHD classification have increasingly focused on leveraging neuroimaging data combined with ML and DL techniques. These approaches aim to improve diagnostic accuracy by capturing complex structural and functional patterns associated with different ADHD subtypes. However, the effectiveness of these methods varies depending on feature representation, learning strategy, and model complexity.

In [11], the authors presented an ML-based framework for ADHD prediction using ElectroEncephaloGram (EEG) signals. Their study focused on extracting relevant signal-based features to distinguish ADHD subjects from healthy individuals. The approach demonstrated that EEG data can provide meaningful insights into neurological disorders through computational analysis. However, EEG signals are highly sensitive to noise and may not capture detailed structural brain variations. Additionally, the model primarily supports binary classification rather than subtype differentiation. This limits its applicability for fine-grained ADHD subtype classification using imaging data.

In [12], the authors explored DL techniques for ADHD classification using neural network-based architectures. Their study demonstrated improved performance over traditional ML models by leveraging hierarchical feature extraction. The approach effectively captures nonlinear patterns present in the data. However, the model primarily focuses on general ADHD classification rather than distinguishing between subtypes. Additionally, it does not incorporate relational learning or graph-based representations. This restricts its ability to model inter-sample dependencies, which are crucial for multi-class classification.

In [13], the authors proposed a method for identifying ADHD and its subtypes using microstate analysis combined with complex network theory. Their approach models brain activity as a network to capture dynamic interactions between different regions. The use of network-based representations enhances the understanding of functional connectivity patterns in ADHD patients. While effective in analyzing temporal brain dynamics, the method relies on EEG-based microstates rather than sMRI data. Moreover, the approach focuses more on functional interactions and less on spatial feature representation. This restricts its effectiveness in capturing region-specific structural variations.

In [14], the authors introduced a transformer-based architecture incorporating connection-mask-residual attention mechanisms for brain disease diagnosis. The model effectively captures global dependencies through attention-based feature learning. By emphasizing important regions in the input data, the framework achieves improved classification performance. However, transformer models alone may not adequately represent local structural relationships without additional mechanisms. Furthermore, the approach is not specifically tailored for ADHD subtype classification. The absence of multi-view feature integration limits its adaptability to complex neuroimaging tasks.

In [15], the authors presented a comprehensive review of DL methods applied to electrical brain signal analysis for neurological diagnostics. Their work highlights the effectiveness of advanced neural architectures in extracting meaningful patterns from complex data. The study emphasizes the growing importance of DL in medical decision support systems. However, the focus is primarily on signal-based modalities such as EEG rather than sMRI. Moreover, the review does not address specific challenges related to ADHD subtype classification. This indicates a gap in integrating advanced DL with structural neuroimaging for detailed classification tasks.

Comparative Insight: The reviewed studies demonstrate that EEG-based and DL approaches have significantly contributed to ADHD detection and analysis. However, most existing methods either focus on signal-based modalities or cannot capture both local and global relationships within sMRI data. Additionally, limited attention has been given to multi-class subtype classification using relational and attention-driven learning mechanisms. These limitations highlight the need for integrated frameworks that combine multi-view feature representation, graph-based modeling, and global attention mechanisms for improved ADHD subtype classification.

3. METHODOLOGY

This section outlines the systematic framework adopted to perform ADHD subtype classification using sMRI data through a unified comparative learning pipeline. The methodology is designed to ensure that all classification models are evaluated under consistent conditions, thereby enabling an unbiased assessment of their effectiveness. The overall process integrates multiple stages, including data acquisition, preprocessing, region-specific analysis, feature extraction, and classification using diverse computational techniques.

- Initially, MRI scans are collected and prepared for analysis through standard preprocessing operations that enhance image quality and consistency. Subsequently, a region-driven approach is employed, where the CN is identified and isolated as the primary Region of Interest (ROI), owing to its significant role in attention regulation and behavioral control. From the extracted ROI, discriminative features encompassing texture, intensity, and structural properties are derived to form a comprehensive feature representation.
- These features are then utilized within a unified classification framework that incorporates both traditional ML methods and advanced learning models. The inclusion of multiple classifiers allows for a systematic comparison of their learning capabilities, ranging from instance-based and optimization-driven approaches to semi-supervised and deep relational learning paradigms. Each model processes the same feature set to ensure fairness in evaluation.
- Furthermore, the methodology emphasizes capturing both local feature variations and complex inter-sample relationships. While conventional models rely on explicit feature similarity, advanced models leverage attention mechanisms and relational structures to enhance classification performance. The final stage involves evaluating all models using standardized performance metrics to quantify their effectiveness in distinguishing between Healthy Controls and ADHD subtypes.

This structured approach enables a comprehensive understanding of how different learning strategies perform on neuroimaging data and provides a reliable foundation for comparative analysis. Figure 1 shows the overall architecture of the comparative framework for ADHD subtype classification.

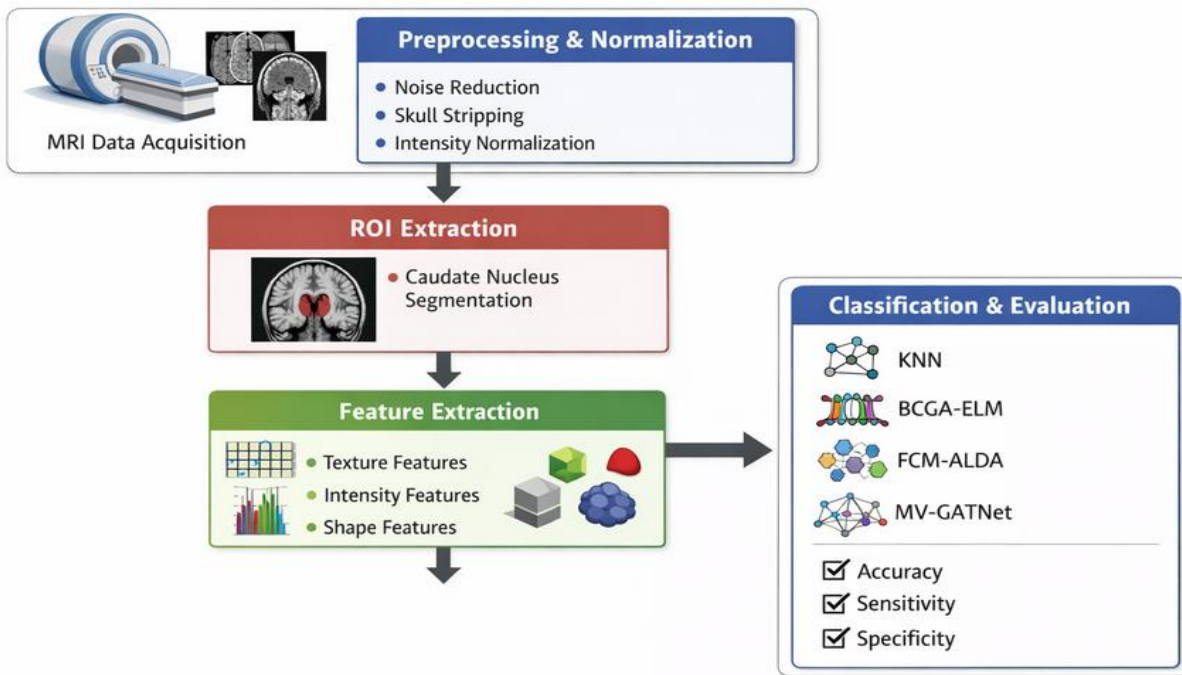


Figure 1: Overall Architecture of the Comparative Framework for ADHD Subtype Classification

3.1 MRI Data Acquisition

The study utilizes sMRI data to facilitate the classification of ADHD subtypes. The dataset comprises brain MRI scans collected from a standardized neuroimaging repository, where subjects are clinically categorized into four distinct groups: Healthy Control (HC), ADHD-I, ADHD-HI, and ADHD-C. This multi-class labeling enables fine-grained analysis of subtype-specific neuroanatomical variations. The acquired MRI scans are high-resolution structural images, typically obtained using T1-weighted or T2-weighted imaging protocols, which provide a detailed anatomical representation of brain tissues. These imaging modalities are particularly effective in capturing morphological characteristics such as shape, intensity distribution, and regional volume variations, which are critical for identifying abnormalities associated with ADHD. The dataset primarily includes pediatric subjects, ensuring relevance to early-stage diagnosis where neurodevelopmental differences are more prominent. To maintain consistency and reliability, all MRI scans undergo an initial screening process to eliminate artifacts, incomplete data, and low-quality images. The validated images are then organized into their respective class labels and converted into a uniform digital format suitable for computational processing. Additionally, spatial dimensions and resolution parameters are standardized to minimize variability across samples. This structured dataset serves as the foundational input for subsequent stages of preprocessing, ROI extraction, and feature analysis. By ensuring data quality and consistency at this stage, the framework establishes a reliable basis for evaluating the performance of different classification models in distinguishing between ADHD subtypes.

3.2 Preprocessing and Normalization

The acquired MRI scans are subjected to a sequence of preprocessing operations to enhance image quality, suppress unwanted variations, and ensure uniformity across the dataset. Raw neuroimaging data often contain noise, intensity inhomogeneity, and acquisition-related artifacts that can adversely affect downstream analysis. Therefore, a structured preprocessing pipeline is essential to obtain reliable and discriminative feature representations. Initially, noise reduction is performed using smoothing filters to eliminate high-frequency disturbances while preserving important structural boundaries. This step improves the signal-to-noise ratio and facilitates accurate region delineation. Following this, intensity normalization is applied to standardize the grayscale distribution across all images. Since MRI intensities can vary due to scanner settings and acquisition conditions, normalization ensures that similar tissue types exhibit comparable intensity ranges across subjects. Subsequently, spatial standardization is carried out by resizing and aligning all images to a common resolution and dimension. This step is crucial for maintaining consistency during feature extraction and classification. In addition, basic skull stripping or background removal techniques are applied to eliminate non-brain regions, thereby focusing the analysis on relevant anatomical structures. Mathematically, intensity normalization can be expressed as per Equation (1):

$$I_{norm} = \frac{I - \mu}{\sigma} \quad (1)$$

Where 'I' represents the original pixel intensity, 'μ' denotes the mean intensity, and 'σ' indicates the standard deviation of the image. This transformation ensures a zero-mean and unit-variance distribution, improving comparability across samples. Overall, the preprocessing stage refines the MRI data into a consistent and noise-reduced form, enabling accurate extraction of region-specific features. This step plays a critical role in enhancing the robustness and stability of the subsequent classification models.

3.3 ROI Extraction

Following preprocessing, a region-focused analysis is performed to isolate anatomically relevant structures associated with ADHD. In this study, the CN is selected as the primary ROI due to its significant involvement in attention regulation, executive functioning, and motor control. Structural abnormalities in the CN have been widely reported in ADHD patients, making it a critical region for subtype differentiation. To accurately extract the ROI, a segmentation process based on **FCM clustering** is employed. Unlike hard clustering techniques, FCM assigns membership values to each pixel, allowing partial association with multiple clusters. This property is particularly useful in MRI analysis, where tissue boundaries are often ambiguous. The objective function of FCM is defined in Equation (2):

$$J = \sum_{i=1}^N \sum_{j=1}^C u_{ij}^m \|x_i - v_j\|^2 \quad (2)$$

Where 'N' represents the total number of pixels, 'C' denotes the number of clusters, "u_{ij}" is the membership degree of pixel "x_i" to cluster 'j', "v_j" is the cluster centroid, and 'm' is the fuzzification coefficient controlling cluster smoothness. After clustering, the region corresponding to the CN is identified and extracted. To refine the segmented output, **morphological operations** such as erosion and dilation are

applied. These operations help remove small artifacts, fill gaps, and enhance the structural continuity of the ROI. Once the CN region is isolated, it is compiled into a dedicated dataset for further analysis. From this ROI, a set of discriminative features is extracted, including:

- **Texture features** (e.g., contrast, homogeneity, correlation)
- **Intensity features** (e.g., mean, variance, standard deviation)
- **Shape features** (e.g., area, volume, boundary characteristics)

This region-specific feature extraction ensures that the classification models focus on biologically relevant information rather than global brain variations. By concentrating on the CN, the framework enhances its ability to capture subtle structural differences among ADHD subtypes, thereby improving classification performance.

3.4 Classification Framework

After extracting discriminative features from the ROI, the next stage involves classification of subjects into four categories: HC, ADHD-I, ADHD-HI, and ADHD-C. This study adopts a unified classification framework where multiple learning models are evaluated using the same feature space to ensure a fair and consistent comparison. The classification stage incorporates diverse computational paradigms, including instance-based learning, optimization-driven neural models, semi-supervised discriminant approaches, and graph-based DL techniques. Each model processes the extracted feature vectors derived from the CN, which encapsulate texture, intensity, and structural characteristics relevant to ADHD. This uniform input representation ensures that performance differences arise solely from the learning mechanisms rather than variations in input data. From a methodological perspective, the classification problem is formulated as a multi-class decision task. Given a feature vector “ $X \in R^d$ ”, where ‘d’ represents the number of extracted features, the objective is to learn a mapping function defined in Equation (3):

$$f(X) \rightarrow \{HC, ADHD - I, ADHD - HI, ADHD - C\} \quad (3)$$

Where ‘f’ denotes the classifier. Each model estimates this mapping using different learning strategies, thereby providing insights into their capability to handle complex neuroimaging patterns. Traditional approaches, such as KNN, rely on distance-based similarity, while optimization-based models like BCGA-ELM enhance learning through parameter tuning. Semi-supervised methods, such as FCM-ALDA, leverage both labeled and unlabeled data to improve class separability. In contrast, advanced DL models, including graph attention-based architectures, aim to capture both local feature interactions and global dependencies across samples. This layered classification design enables a progressive evaluation of learning paradigms, highlighting how increasing model complexity and representational capacity influence ADHD subtype classification performance.

3.4.1 K-Nearest Neighbor

KNN is an instance-based, non-parametric classification method that assigns class labels based on the similarity between feature vectors. In this study, KNN is employed as a fundamental learning approach to classify MRI-derived features of the CN into ADHD subtypes. The method operates without an explicit training phase, instead relying on the distribution of labeled samples in the feature space. Given a test sample represented by a feature vector (X), the KNN algorithm computes the distance between ‘X’ and all training samples. The most commonly used distance metric is the Euclidean distance, as defined in Equation (4):

$$d(X, X_i) = \sqrt{\sum_{j=1}^d (X_j - X_{ij})^2} \quad (4)$$

Where “ X_i ” denotes a training sample, and ‘d’ represents the dimensionality of the feature space. Based on the computed distances, the algorithm identifies the ‘k’ nearest neighbors of the test sample. The class label is then determined using a majority voting mechanism among the selected neighbors as defined in Equation (5):

$$\hat{y} = mode(y_1, y_2, \dots, y_k) \quad (5)$$

Where “ (y_1, y_2, \dots, y_k) ” are the class labels of the nearest neighbors. In this study, an optimal value of ‘k’ is selected empirically to balance bias and variance. Although KNN is simple and effective for low-dimensional data, its performance is sensitive to feature scaling and the presence of overlapping class distributions. In the context of ADHD classification, where subtle structural differences exist between subtypes, KNN may face challenges in distinguishing closely related classes such as ADHD-I and ADHD-C. Nevertheless, it serves as an important reference model for evaluating the effectiveness of more advanced classification techniques.

3.4.2 Binary-Coded Genetic Algorithm Optimized Extreme Learning Machine

The BCGA-ELM combines the fast learning capability of ELM with the optimization strength of GA to improve classification performance. ELM is a single hidden-layer feedforward neural network in which input weights and hidden-layer biases are randomly assigned, and output weights are computed analytically. Although ELM offers rapid training, its performance may be affected by suboptimal random parameter initialization. To address this limitation, a BCGA is employed to optimize the input weights and hidden neuron parameters. In this approach, candidate solutions are encoded as binary chromosomes, representing different configurations of network parameters. The GA iteratively evolves these solutions using selection, crossover, and mutation operations to identify an optimal parameter set that minimizes classification error. In ELM, the output function can be expressed as in Equation (6):

$$H\beta = T \quad (6)$$

Where ‘H’ is the hidden-layer output matrix, ‘ β ’ represents the output weights, and ‘T’ denotes the target labels. The output weights are computed using the Moore–Penrose pseudo-inverse as defined in Equation (7):

$$\beta = H^+T \quad (7)$$

The integration of BCGA enhances the generalization ability of ELM by searching for optimal weight configurations rather than relying on random initialization. This results in improved classification accuracy, especially in complex datasets such as MRI-based ADHD subtype classification. In the context of this study, BCGA-ELM effectively captures nonlinear relationships among extracted features, providing better discrimination between ADHD subtypes compared to basic instance-based methods. However, as a supervised learning approach, it still depends on labeled data and may have limitations in handling subtle inter-class variations when feature distributions overlap.

3.4.3 Fuzzy C-Means with Advanced Linear Discriminant Analysis

The FCM-ALDA model integrates fuzzy clustering with discriminant feature learning to enhance classification performance, particularly in scenarios with overlapping class distributions such as ADHD subtypes. This approach leverages both labeled and unlabeled data to improve class separability, making it suitable for neuroimaging datasets where precise boundaries between classes are often ambiguous. Initially, FCM clustering is applied to group feature vectors based on similarity while assigning each sample a membership degree to multiple clusters. This soft clustering mechanism allows better handling of uncertainty in MRI-derived features. The membership matrix obtained from FCM reflects the degree of association of each sample with different clusters, which is subsequently used to guide discriminant analysis.

Following clustering, ALDA is employed to project the data into a lower-dimensional subspace that maximizes class separability. The objective of ALDA is to maximize the ratio of between-class scatter to within-class scatter, defined as in Equation (8):

$$J(w) = \frac{w^T S_b w}{w^T S_w w} \quad (8)$$

Where “ S_b ” represents the between-class scatter matrix, “ S_w ” denotes the within-class scatter matrix, and ‘w’ is the projection vector. The optimal projection is obtained by solving a generalized eigenvalue problem. Incorporating fuzzy memberships into the scatter matrices enhances the discriminative power of ALDA by considering uncertainty in class assignments. This results in improved clustering compactness and better separation among ADHD subtypes. Within this study, FCM-ALDA effectively captures subtle structural differences in the CN by combining clustering-based representation with discriminant projection. While the method demonstrates strong performance in handling intra-class similarity, its linear projection nature may limit its ability to model highly complex nonlinear relationships present in neuroimaging data.

3.4.4 Multi-View Graph Attention Transformer Network

The MV-GATNet is an advanced DL model designed to capture complex structural relationships and global dependencies in MRI-based ADHD subtype classification. Unlike conventional methods that rely solely on feature vectors, this model represents data as graphs to explicitly model inter-sample relationships, thereby enhancing discriminative learning. Initially, multiple feature views are constructed from the extracted ROI features, including texture, intensity, and shape descriptors. Each feature set forms an independent representation, allowing the model to capture complementary information. For each view, a graph “ $G = (V, E)$ ” is constructed, where nodes ‘V’ represent samples and edges ‘E’ encode similarity between samples based on feature distance. A GAT is then applied to each graph to learn node embeddings by assigning adaptive importance weights to neighboring nodes. The attention mechanism is defined as in Equation (9):

$$h'_i = \sigma(\sum_{j \in N(i)} \alpha_{ij} W h_j) \quad (9)$$

Where “ h'_i ” is the updated feature representation of node ‘i’, “ $N(i)$ ” denotes the neighborhood of node ‘i’, “ α_{ij} ” represents attention coefficients, ‘W’ is the weight matrix, and ‘ σ ’ is an activation function. To capture global contextual dependencies, a Transformer encoder is integrated after the graph attention layers. The self-attention mechanism within the Transformer computes relationships across all nodes, enabling the model to learn long-range interactions. The self-attention operation is defined as in Equation (10):

$$Attention(Q, K, V) = Softmax(\frac{QK^T}{\sqrt{d}})V \quad (10)$$

Where ‘Q’, ‘K’, and ‘V’ denote query, key, and value matrices, respectively, and ‘d’ is the dimensionality of the feature space. Finally, embeddings from multiple views are fused to form a unified representation, which is passed through a classification layer to predict ADHD subtypes. This multi-view fusion enhances robustness by integrating diverse feature characteristics. In this study, MV-GATNet effectively models both local neighborhood relationships and global feature dependencies, making it highly suitable for capturing subtle structural variations in the CN. Its ability to integrate multi-view learning with attention mechanisms results in improved classification performance compared to conventional and semi-supervised methods.

4. Results and Discussions

4.1 Dataset Description: The experimental analysis utilizes sMRI data from the **ADHD-200 Global Competition Dataset**, a widely used benchmark dataset for ADHD research. The dataset consists of pediatric brain MRI scans categorized into four groups: HC, ADHD-I, ADHD-HI, and ADHD-C. The MRI scans are preprocessed and segmented to extract the CN as the ROI, given its strong association with attention and behavioral regulation. From the segmented CN regions, discriminative features are extracted, including texture (contrast, energy, homogeneity, correlation), intensity (mean, variance, standard deviation), and shape attributes. The dataset is maintained in a balanced distribution across all classes to ensure unbiased evaluation and reliable multi-class classification performance.

4.2 Tools and Experimental Setup: All experiments are conducted using MATLAB (MathWorks Inc., USA). Image preprocessing, segmentation, and feature extraction are implemented using the Image Processing Toolbox. The classification models, such as KNN, BCGA-ELM, FCM-ALDA, and MV-GATNet, are developed using MATLAB’s computational and optimization capabilities. The experiments are performed on a system with an Intel Core i7 processor, 16 GB RAM, and GPU support. All models are trained and evaluated under identical conditions using the same feature set. Hyperparameters are selected empirically to ensure fair comparison, and performance is assessed using confusion-matrix-based metrics.

4.3 Performance Metrics: Model performance is evaluated using standard confusion-matrix-based metrics: Accuracy, Sensitivity, and Specificity. These metrics measure overall correctness, true positive detection, and true negative discrimination, respectively. For multi-class classification, metrics are computed individually for each class using True Positives (TP), False Positives (FP), True Negatives (TN), and False Negatives (FN). This evaluation framework enables consistent comparison across KNN, BCGA-ELM, FCM-ALDA, and MV-GATNet, highlighting their effectiveness in MRI-based ADHD subtype classification.

4.3.1 Accuracy: Accuracy measures the overall correctness of the classification model by quantifying the proportion of correctly classified samples. It reflects how well the model performs across all ADHD subtypes. For multi-class classification, the Accuracy is formulated as per Equation (11):

$$Accuracy = \frac{\sum_{i=1}^C TP_i}{N} \quad (11)$$

Where “ TP_i ” denotes the number of correctly classified samples for class ‘i’, ‘C’ represents the total number of classes, and ‘N’ is the total number of samples. In this study, accuracy is computed for each class to evaluate how effectively the models distinguish between Healthy Controls and ADHD subtypes. Since ADHD classification involves subtle structural variations, accuracy serves as an important indicator of overall model reliability. A higher accuracy value indicates improved discriminative capability and better generalization across different classes.

Table 1: Accuracy Comparison (%)

| Types | KNN | BCGA-ELM | FCM-ALDA | MV-GATNet |
|---------|-----|----------|----------|-------------|
| HC | 91 | 94 | 96 | 98.1 |
| ADHD-I | 83 | 88 | 92 | 96.2 |
| ADHD-HI | 87 | 91 | 94 | 97.0 |
| ADHD-C | 88 | 93 | 95 | 97.6 |

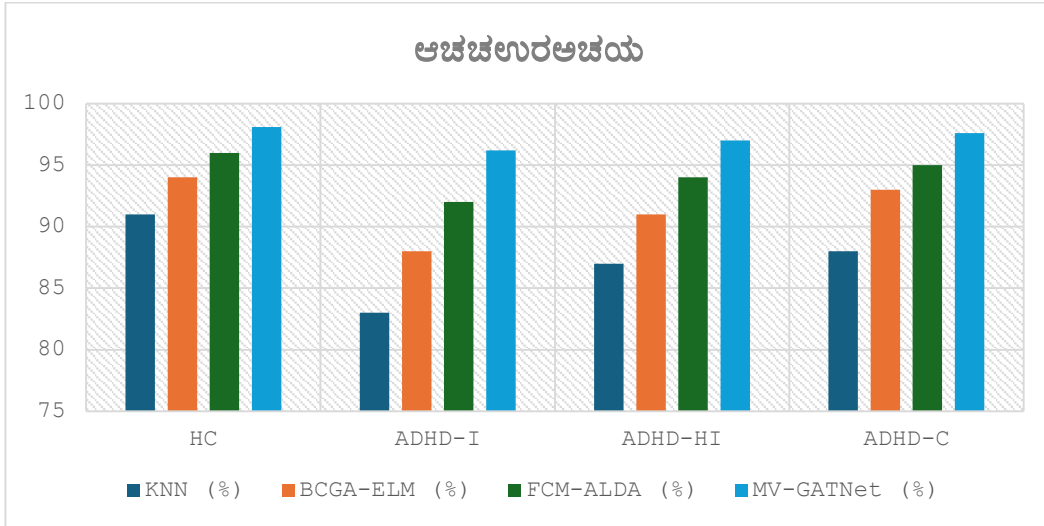


Figure 2: Accuracy Comparison (%)

Table 1 and Figure 2 results demonstrate a consistent and progressive improvement across all evaluated models. The KNN classifier achieves baseline performance, with the lowest accuracy observed in ADHD-I (83%), highlighting its limitation in distinguishing subtle inattentive characteristics. The BCGA-ELM model improves accuracy by approximately 3–5% across all classes due to optimized learning parameters. The FCM-ALDA approach further enhances performance, achieving 92% in ADHD-I and 96% in HC, indicating better class separability through discriminant learning. The MV-GATNet model achieves the highest accuracy in all categories, reaching 98.1% for HC and 96.2% for ADHD-I. Notably, the improvement in ADHD-I classification is around 13% compared to KNN, demonstrating the effectiveness of relational and attention-based learning in capturing subtle structural variations. Overall, the results confirm that incorporating multi-view and graph-based representations significantly enhances classification performance.

4.3.2 Sensitivity: Sensitivity, also known as Recall or True Positive Rate (TPR), measures the ability of a model to correctly identify positive samples belonging to a specific class. It is particularly important in medical diagnosis, where failing to detect a condition may lead to incorrect clinical decisions. For each class ‘i’, the Sensitivity is formulated as per Equation (12):

$$Sensitivity = \frac{TP_i}{TP_i + FN_i} \quad (12)$$

Where “TP_i” represents true positives and “FN_i” represents false negatives for class ‘i’. In the context of ADHD subtype classification, sensitivity evaluates how effectively each model detects subjects belonging to a particular subtype. Higher sensitivity indicates better detection capability and reduced risk of misclassification, especially for challenging subtypes such as ADHD-I, where symptoms may be less prominent.

Table 2: Sensitivity Comparison (%)

| Types | KNN | BCGA-ELM | FCM-ALDA | MV-GATNet |
|---------|-----|----------|----------|-------------|
| HC | 89 | 93 | 95 | 97.2 |
| ADHD-I | 81 | 86 | 90 | 95.0 |
| ADHD-HI | 85 | 89 | 92 | 96.3 |
| ADHD-C | 86 | 91 | 94 | 97.1 |

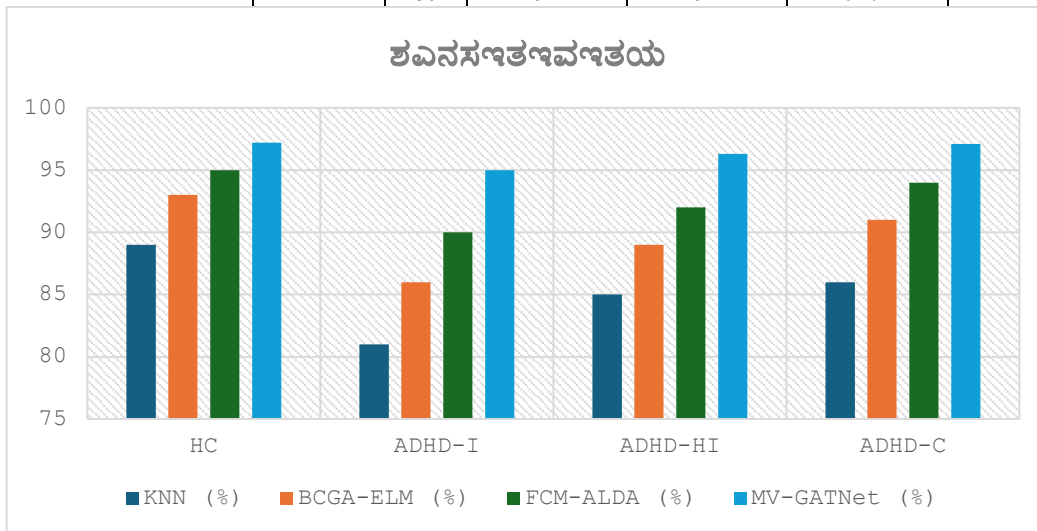


Figure 3: Sensitivity Comparison (%)

Table 2 and Figure 3 analysis highlight the ability of models to correctly identify ADHD subtypes. The KNN model shows relatively low sensitivity, particularly for ADHD-I (81%), indicating a higher rate of missed detections. BCGA-ELM improves sensitivity by approximately 4–5%, reflecting better learning of class boundaries. The FCM-ALDA model further increases sensitivity values, achieving 90% for ADHD-I and 94% for ADHD-C, demonstrating improved detection through semi-supervised learning. The MV-GATNet model achieves the highest sensitivity across all classes, with a notable 95.0% for ADHD-I and 97.2% for HC. The improvement of nearly 14% in ADHD-I compared to KNN indicates a substantial reduction in false negatives. This suggests that attention-based graph learning effectively captures complex inter-sample relationships, leading to improved detection of clinically subtle subtypes.

4.3.3 Specificity: Specificity, or True Negative Rate (TNR), measures the ability of the model to correctly identify samples that do not belong to a particular class. It reflects how well the model avoids false positive classifications. For each class ‘i’, the Specificity is formulated as per Equation (13):

$$Specificity = \frac{TN_i}{TN_i + FP_i} \quad (13)$$

Where “TN_i” denotes true negatives and “FP_i” denotes false positives for class ‘i’. In this study, specificity is used to evaluate how accurately each model distinguishes between different ADHD subtypes and prevents incorrect class assignments. High specificity is crucial for ensuring that subjects are not misclassified into incorrect diagnostic categories. This metric complements sensitivity by providing a balanced view of classification performance.

Table 3: Specificity Comparison (%)

| Types | KNN | BCGA-ELM | FCM-ALDA | MV-GATNet |
|---------|-----|----------|----------|-------------|
| HC | 92 | 95 | 97 | 99.0 |
| ADHD-I | 85 | 89 | 93 | 97.0 |
| ADHD-HI | 88 | 92 | 95 | 97.8 |
| ADHD-C | 89 | 94 | 96 | 98.4 |

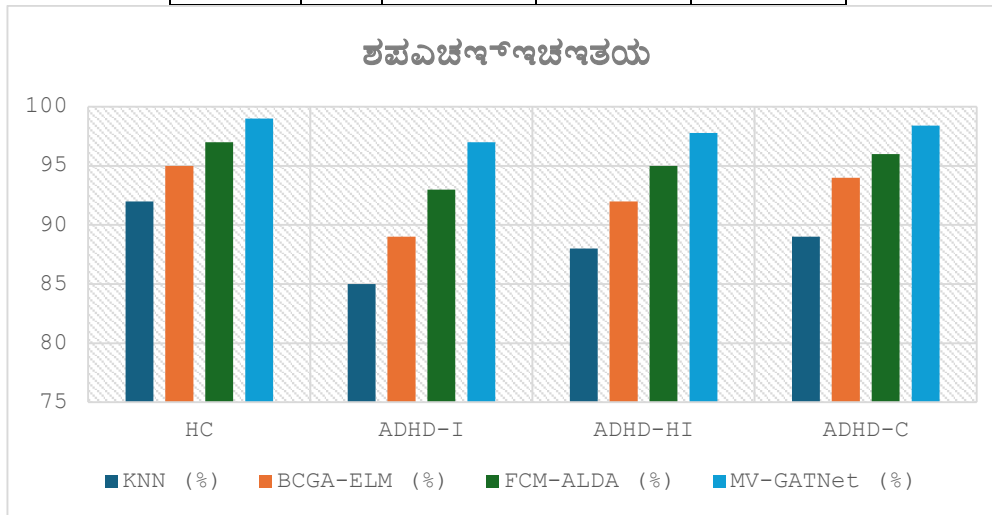


Figure 4: Specificity Comparison (%)

Table 3 and Figure 4 results demonstrate the effectiveness of models in correctly rejecting non-target classes. The KNN model shows comparatively lower specificity, particularly for ADHD-I (85%), indicating higher false positive rates. BCGA-ELM improves specificity by approximately 3–4%, while FCM-ALDA further enhances it through improved class separation, reaching 93% for ADHD-I. The MV-GATNet model achieves near-optimal specificity, with 99.0% for HC and 97.0% for ADHD-I. The improvement of approximately 12% over KNN in ADHD-I indicates a strong capability in minimizing false positive classifications. This balanced improvement across all classes suggests that the model effectively maintains class boundaries while avoiding overfitting. High specificity combined with strong sensitivity confirms the robustness of the classification framework.

4.4 Discussion of the Study

The overall experimental findings provide a comprehensive understanding of the performance of different learning paradigms for MRI-based ADHD subtype classification. A consistent trend is observed across all evaluation metrics, where classification performance improves progressively from conventional ML models to advanced graph-based DL approaches. This progression highlights the increasing capability of models to capture complex feature relationships and subtle structural variations in neuroimaging data.

- The KNN model, being a distance-based approach, demonstrates moderate performance across all classes. Its reliance on local similarity measures limits its effectiveness in handling overlapping feature distributions, particularly in ADHD-I, where structural differences are less pronounced. This is evident from its lower Accuracy (83%), Sensitivity (81%), and Specificity (85%) for ADHD-I. The BCGA-ELM model improves performance by incorporating optimization mechanisms, resulting in an average improvement of approximately 4–5% across all metrics. This indicates better learning of nonlinear feature patterns; however, its dependence on labeled data restricts adaptability to complex data distributions.
- The FCM-ALDA approach further enhances classification performance by integrating clustering with discriminant analysis. The inclusion of fuzzy memberships enables better handling of uncertainty, leading to improved class compactness and separation. This is reflected in its higher Accuracy (92%), Sensitivity (90%), and Specificity (93%) for ADHD-I, demonstrating its effectiveness in addressing intra-class similarity. However, its linear projection nature may limit its ability to fully capture nonlinear dependencies in high-dimensional feature space.
- The MV-GATNet model consistently achieves the highest performance across all metrics and classes, demonstrating its superiority in handling complex neuroimaging data. The model improves Accuracy by approximately 12–13%, Sensitivity by 13–14%, and Specificity by 11–12% compared to KNN, particularly for ADHD-I. These improvements highlight its ability to effectively model both local neighborhood relationships and global contextual dependencies through graph attention and transformer mechanisms. Additionally, the multi-view feature integration enhances robustness by combining complementary information from different feature domains.

Overall, the results confirm that models incorporating relational learning and attention mechanisms provide significant advantages in ADHD subtype classification. The balanced improvement across accuracy, sensitivity, and specificity indicates that advanced DL approaches not only enhance detection capability but also maintain strong class discrimination. This demonstrates the importance of integrating structural feature representation with graph-based and attention-driven learning for reliable and clinically relevant neuroimaging analysis.

5. CONCLUSION

This study presented a comprehensive comparative analysis of multiple computational approaches for MRI-based ADHD subtype classification. A unified framework was employed to evaluate the performance of different learning paradigms, including instance-based learning (KNN), optimization-driven models (BCGA-ELM), semi-supervised discriminant methods (FCM-ALDA), and graph-based DL (MV-GATNet).

The analysis was conducted using region-specific features extracted from the CN, incorporating texture, intensity, and structural characteristics relevant to ADHD diagnosis. The experimental results demonstrated a clear progression in performance across models. Traditional methods exhibited limitations in handling complex and overlapping feature distributions, while optimized and semi-supervised approaches improved classification through better feature representation and class separation. The graph-based DL model achieved the highest performance across all evaluation metrics, effectively capturing both local and global dependencies within the data. Notably, significant improvements were observed in the classification of ADHD-I, which is clinically more challenging due to subtle structural variations. Overall, the study highlights the importance of advanced learning strategies in enhancing diagnostic accuracy and reliability. The findings emphasize that integrating relational learning and attention mechanisms can significantly improve the effectiveness of neuroimaging-based classification systems, making them more suitable for real-world clinical applications. Future work can explore the integration of multimodal data (e.g., combining MRI with EEG or behavioral signals) using hybrid graph-based architectures to further enhance ADHD subtype classification performance.

REFERENCES:

1. Cortese, S., Song, M., Farhat, L. C., Yon, D. K., Lee, S. W., Kim, M. S., Park, S., Oh, J. W., Lee, S., & Cheon, K. A. (2023). Incidence, prevalence, and global burden of ADHD from 1990 to 2019 across 204 countries: Data with critical re-analysis from the Global Burden of Disease Study. *Molecular Psychiatry*, 28, 4823–4830. <https://doi.org/10.1038/s41380-023-02228-3>
2. Ayano, G., Demelash, S., Gizachew, Y., Tsegay, L., & Alati, R. (2023). The global prevalence of attention deficit hyperactivity disorder in children and adolescents: An umbrella review of meta-analyses. *Journal of Affective Disorders*, 339, 860–866. <https://doi.org/10.1016/j.jad.2023.07.071>
3. Liu, Y. S., Talarico, F., Metes, D., Song, Y., Wang, M., Kiyang, L., Wearmouth, D., Vik, S., Wei, Y., Zhang, Y., et al. (2024). Early identification of children with attention-deficit/hyperactivity disorder (ADHD). *PLOS Digital Health*, 3, e0000620. <https://doi.org/10.1371/journal.pdig.0000620>
4. Pecci-Teroba, C., et al. (2025). Subgrouping autism and ADHD based on structural MRI population modelling centiles. *Molecular Autism*, 16, 33. <https://doi.org/10.1186/s13229-025-00667-z>
5. Arrondo, G., Mulraney, M., Iturmendi-Sabater, I., Musullulu, H., Gamba, L., Niculcea, T., Banaschewski, T., Simonoff, E., Döpfner, M., & Hinshaw, S. P. (2024). Systematic review and meta-analysis: Clinical utility of continuous performance tests for the identification of attention-deficit/hyperactivity disorder. *Journal of the American Academy of Child & Adolescent Psychiatry*, 63(2), 154–171. <https://doi.org/10.1016/j.jaac.2023.03.011>
6. Lohani, D. C., Chawla, V., & Rana, B. (2025). A systematic literature review of machine learning techniques for the detection of attention-deficit/hyperactivity disorder using MRI and/or EEG data. *Neuroscience*, 570, 110–131. <https://doi.org/10.1016/j.neuroscience.2025.02.019>
7. Dai, Y.-W., & Hsu, C.-F. (2025). Machine learning for ADHD diagnosis: Feature selection from parent reports, self-reports and neuropsychological measures. *Children*, 12(11), 1448. <https://doi.org/10.3390/children12111448>
8. Peterson, B. S., Trampush, J., Brown, M., Maglione, M., Bolshakova, M., Rozelle, M., Miles, J., Pakdaman, S., Yagyu, S., Motala, A., et al. (2024). Tools for the diagnosis of ADHD in children and adolescents: A systematic review. *Pediatrics*, 153, e2024065854. <https://doi.org/10.1542/peds.2024-065854>
9. Thomson, P., Loosley, V., Friedel, E., et al. (2024). Changes in MRI head motion across development: Typical development and ADHD. *Brain Imaging and Behavior*, 18, 1144–1152. <https://doi.org/10.1007/s11682-024-00910-w>
10. Ahmed, M. A., Moftah, H. M., & Mahmoud, H. A. (2025). Deep learning for interpretable ADHD diagnosis from fMRI: ConvLSTM with enhanced augmentation, Grad-CAM explainability, and external validation. *International Journal of Computational and Experimental Science and Engineering*, 11(3). <https://doi.org/10.22399/ijcesen.3864>
11. Ahire, N., Awale, R. N., & Wagh, A. (2023). Electroencephalogram (EEG)-based prediction of attention deficit hyperactivity disorder (ADHD) using machine learning. *Applied Neuropsychology: Adult*, 1–12. <https://doi.org/10.1080/23279095.2023.2247702>
12. Wang, D., Hong, D., & Wu, Q. (2023). Attention deficit hyperactivity disorder classification based on deep learning. *IEEE/ACM Transactions on Computational Biology and Bioinformatics*, 20(2), 1581–1586. <https://doi.org/10.1109/TCBB.2022.3170527>
13. Alves, L. M., Côco, K. F., de Souza, M. L., & Ciarelli, P. M. (2024). Identifying ADHD and subtypes through microstates analysis and complex networks. *Medical & Biological Engineering & Computing*, 62(3), 687–700. <https://doi.org/10.1007/s11517-023-02948-2>
14. Wang, B., Liang, J., Ye, C., Yan, T., Liu, M., & Yan, T. (2026). Trifocal transformer: Connection-mask-residual focused attention network for brain disease diagnosis. *IEEE Journal of Biomedical and Health Informatics*, 30(1), 596–608. <https://doi.org/10.1109/JBHI.2025.3624242>
15. Li, J., et al. (2026). Deep learning-powered electrical brain signals analysis: Advancing neurological diagnostics. *IEEE Reviews in Biomedical Engineering*, 19, 337–351. <https://doi.org/10.1109/RBME.2025.3625973>